Water Quality and Ecosystem Modeling, 1, 193–222, 2000

Modeling Sediment Transport Dynamics in Thompson Island Pool, Upper Hudson River

C. KIRK ZIEGLER kziegler@qeallc.com
Quantitative Environmental Analysis, LLC, 305 West Grand Avenue, Montvale, NJ 07645

PETER H. ISRAELSSON
Quantitative Environmental Analysis, LLC, 305 West Grand Avenue, Montvale, NJ 07645

JOHN P. CONNOLLY
Quantitative Environmental Analysis, LLC, 305 West Grand Avenue, Montvale, NJ 07645

Abstract. Two-dimensional, vertically-averaged hydrodynamic and sediment transport models were developed and applied as part of a PCB fate and transport modeling study of Thompson Island Pool (TIP), Upper Hudson River. Mechanistic formulations were used to simulate cohesive and non-cohesive suspended load transport; site-specific data were extensively used to determine model inputs. This modeling approach is compared and contrasted to non-mechanistic solids transport sub-models used in other contaminant fate studies. A minimum number of model parameters were adjusted to calibrate the sediment transport model using data collected during the 1994 spring flood. The model was validated during the 1997 spring flood and for a 22-year (1977-1998) period. Successful calibration and validation of the model showed that: (1) deposition and resuspension processes were realistically and accurately formulated in the model; (2) the model is an effective diagnostic tool for quantitatively evaluating net deposition and erosion from various areas of TIP; and (3) sediment transport results can be coupled with a PCB fate model with a high degree of confidence.

Keywords: Sediment transport, modeling, Upper Hudson River

1. Introduction

Over an approximate 30-year period, ending in 1977, two General Electric (GE) capacitor manufacturing facilities in Fort Edward and Hudson Falls, New York discharged wastewater containing polychlorinated biphenyls (PCBs) into the Upper Hudson River (UHR). Much of the PCBs accumulated in the sediments upstream of the former Fort Edward Dam located approximately 3 km downstream of the Hudson Falls capacitor plant. Removal of this dam in 1973 and subsequent high flow events resulted in the movement of large quantities of PCB-containing sediments downstream. Some of these sediments deposited further downstream in pools formed by dams along the Champlain Canal, which is coincident with the UHR channel. Most of the historically-deposited, sediment-associated PCBs are now sequestered below the sediment surface, a consequence of the continual deposition of watershed-derived particulate matter. However, the contaminated bed sediments near or at the sediment surface are an "active" source of PCBs to the water column and to biota.

In 1990, the U.S. Environmental Protection Agency (USEPA) began a reassessment of the 1984 "No Action" decision for the sediments in the UHR. Recognizing the complexity and dynamic nature of the links between the sediment PCB levels and PCB levels in the

water column and biota, GE undertook the development of a mass balance model. The purpose of the model is to provide scientifically reliable estimates of future PCB levels within the river. The model framework consists of four sub-models: hydrodynamic; sediment transport; PCB fate and transport; and PCB bioaccumulation. The hydrodynamic and sediment transport models will be the focus of this paper. A complete description of the modeling framework is presented in QEA (1999); an on-line copy of this report is located at www.hudsonwatch.com. The PCB fate model is described in Connolly et al. (2000).

Sediment transport processes are controlling factors in the fate and transport of PCBs in the UHR. Natural recovery in the river is primarily controlled by sedimentation, which is affected by resuspension and deposition processes, as well as sediment loading. Bed erosion during a rare flood event, e.g., 100-year flood, which could possibly cause elevated bed PCB concentrations buried at depth to be introduced back into the bioavailable zone, is determined by hydrodynamic processes and properties of the sediment bed. Thus, understanding and quantifying sediment transport processes is of critical importance when evaluating PCB fate in the river and the effectiveness of various remedial alternatives.

Many previous contaminant fate and transport modeling studies have used solids transport sub-models that are relatively simplistic, non-mechanistic, empirical and poorly constrained. This type of model has generally produced unsatisfactory results, largely because of inadequacies in the sediment transport sub-model. In the study described in this paper, a mechanistic sediment transport model has been applied to the UHR, with sediment transport results being transferred to a PCB fate model (Connolly et al., 2000). One objective of this paper is to provide a description of the development, calibration and validation of the hydrodynamic and sediment transport sub-models in order to demonstrate the scientific credibility of the model. Two additional goals of this paper are: 1) provide a discussion of data analyses and modeling techniques that are used to develop and apply a relatively sophisticated, mechanistic sediment transport model; and 2) contrast the current effort with previous studies that have used non-mechanistic approaches. This discussion will hopefully aid other modelers that are using contaminant fate models and make it possible to improve the predictive capability and reliability of future models.

2. Description of Study Area

The UHR is a run-of-the-river reservoir system, comprised of a series of eight dams and associated backwaters, which extends from Fort Edward to Troy, New York, a distance of approximately 64 km. Hydrodynamic and sediment transport models have been developed, calibrated and validated for each of the eight reaches in the UHR (QEA, 1999). This paper describes the hydrodynamic and sediment transport models developed for Thompson Island Pool (TIP), which is the first reach downstream of Fort Edward. TIP is the pool immediately downstream of Fort Edward, and it has a length of 9.6 km. This reach of the UHR is the region of principal focus of the USEPA reassessment because the highest UHR PCB concentrations, in the bed and biota, are found in TIP. In addition, comprehensive data sets, spanning more than 20 years, are available for this reach, making it possible to adequately calibrate and validate all four sub-models.

TIP extends from Fort Edward to its termination at Thompson Island Dam, which is an uncontrolled, low-head dam that is 1.2 m high (Figure 1). The average width of TIP is 210 m and this reach has a surface area of 200 ha. The mean water depth in this reach is about 3 m, with significant lateral variability in depth due to the Champlain Canal navigational channel. The central channel of the river, which has been dredged in the past, has maximum depths of 6-7 m. Shallower, nearshore areas typically have depths of 1-2 m. Generally, the sediment bed in the deeper central channel areas is primarily composed of sand, gravel and rock; cohesive sediment deposits are usually located in the shallower, nearshore areas.

The mean flow rate of the UHR at Fort Edward is 147 m^3/s, with the average flow rate at the dam higher than this by about 6 m^3/s. The flow increase is due to tributary and direct drainage flow into TIP from a 417 km^2 drainage basin. Approximately 80% of the total runoff comes from two primary tributaries (Snook Kill and Moses Kill), with the balance of the runoff from smaller creeks and direct runoff.

3. Hydrodynamic Model

Inclusion of this sub-model in any contaminant fate model is important because of the dependence of sediment resuspension and deposition on bottom shear stress, which is calculated by the hydrodynamic model. Typically, hydrodynamic models have not been coupled to contaminant fate models; past contaminant fate models have generally relied on simple flow routing techniques and have not calculated bottom shear stress (e.g., O'Connor et al., 1983; Velleux and Endicott, 1994). This simplistic representation of hydrodynamic processes should not be used. A hydrodynamic model is required in order to adequately simulate temporal and spatial variations in current velocity, water depth and bottom shear stress. The level of complexity that is needed, i.e., a one-, two- or three-dimensional hydrodynamic model, will depend on the geometry and flow conditions in a particular aquatic system and the degree of accuracy required for the study.

TIP is relatively shallow and its flow is unstratified. These conditions make it reasonable to assume that the water column is vertically well-mixed. Thus, the two-dimensional, vertically-averaged equations are an accurate approximation to the general three-dimensional equations of motion for an incompressible fluid. The conservation of mass and momentum equations applied to TIP are (Ziegler and Nisbet, 1994)

$$\frac{\partial \eta}{\partial t} + \frac{\partial (uh)}{\partial x} + \frac{\partial (vh)}{\partial y} = 0 \tag{1}$$

$$\frac{\partial (uh)}{\partial t} + \frac{\partial (u^2 h)}{\partial x} + \frac{\partial (uvh)}{\partial y} = -gh\frac{\partial \eta}{\partial x} - C_f q u + \frac{\partial}{\partial x}\left(hB_H \frac{\partial u}{\partial x}\right) + \frac{\partial}{\partial y}\left(hB_H \frac{\partial u}{\partial y}\right) \tag{2}$$

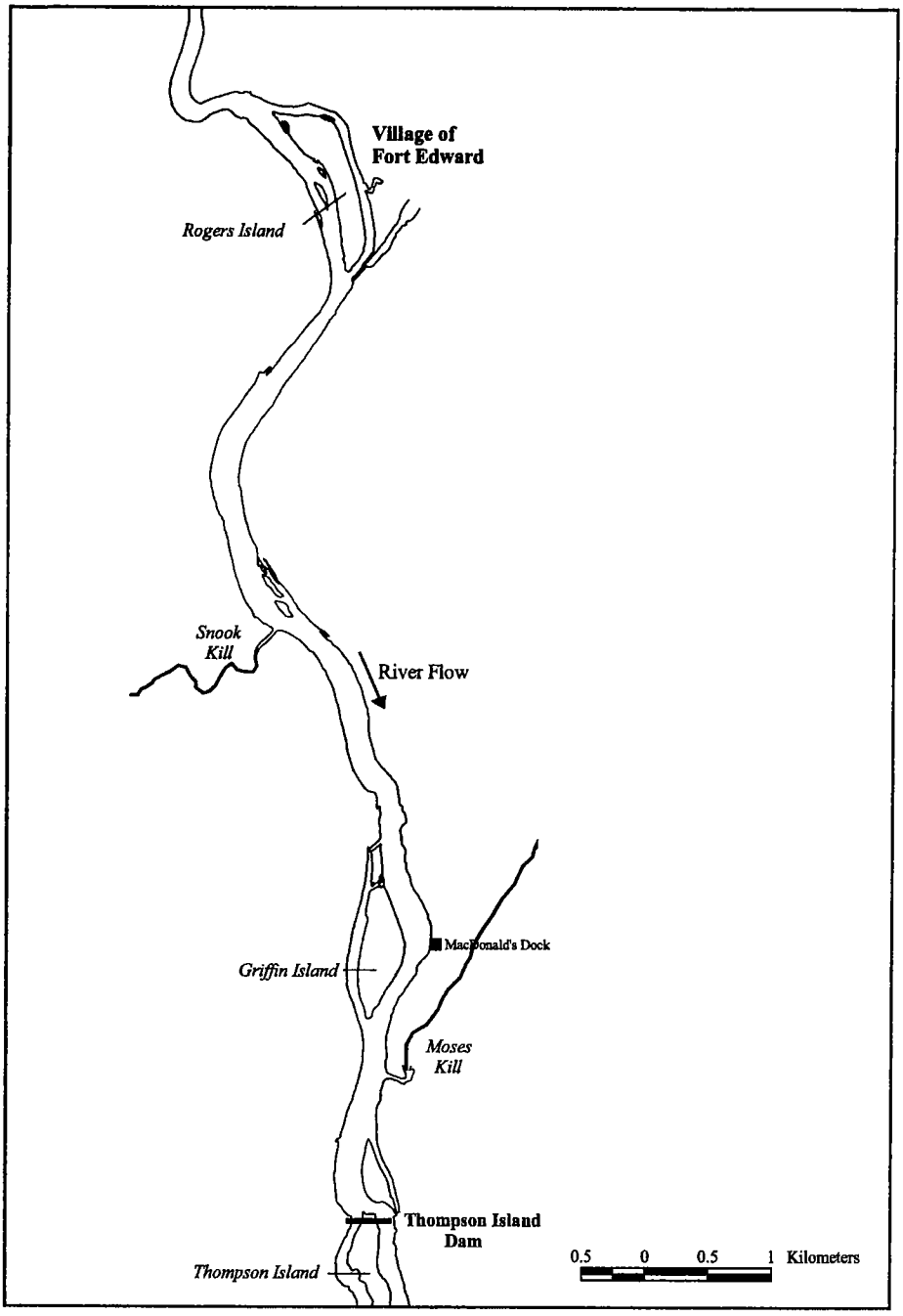

Figure 1. Thompson Island Pool, Upper Hudson River.

$$\frac{\partial(vh)}{\partial t}+\frac{\partial(uvh)}{\partial x}+\frac{\partial(v^2h)}{\partial y}=-gh\frac{\partial\eta}{\partial y}-C_fqv+\frac{\partial}{\partial x}\left(hB_H\frac{\partial v}{\partial x}\right)+\frac{\partial}{\partial y}\left(hB_H\frac{\partial v}{\partial y}\right) \quad (3)$$

where the total water depth is $h = h_o + \eta$; h_o = reference water depth; η = water surface displacement with respect to reference depth; u, v = velocities along the x- and y-axes, respectively; $q = (u^2 + v^2)^{1/2}$; C_f = spatially variable bottom friction factor; and B_H = horizontal eddy viscosity. Note that the x-axis is oriented in the longitudinal (along-channel) direction and the y-axis is oriented in the lateral (cross-channel) direction. Equations (1) to (3) were transformed from Cartesian coordinates to orthogonal, curvilinear coordinates in order to resolve more accurately the complex geometry and bathymetry of TIP. The resulting equations were solved numerically using the semi-implicit version of a well-established hydrodynamic model, ECOM (Blumberg, 1994).

The bottom friction factor in Equations (2) and (3) is dependent on the local water depth and effective bottom roughness (Blumberg and Mellor, 1983)

$$C_f = MAX\left[\frac{\kappa^2}{\left(\ln\frac{h}{2z_o}\right)^2}, C_{f,\min}\right] \quad (4)$$

where κ = von Karman's constant (0.4); $C_{f,\min}$ = minimum bottom friction factor; and z_o = effective bottom roughness. The bottom friction factor (C_f) thus varies both spatially and temporally due to changes in total water depth (h) and bottom roughness (z_o). Spatial variations in bottom roughness are included by using different z_o values for cohesive and non-cohesive sediment bed types. It was assumed that bottom roughness in non-cohesive and hard bottom areas (which used the same z_o value) is greater than z_o in cohesive bed areas, which is consistent with the physical characteristics of those two bed types. Cohesive beds are hydraulically smoother than non-cohesive beds because: (1) median sediment particle diameter (d_{50}) is lower and (2) bed forms tend to be absent or significantly smaller.

The model extends from Route 197 bridge at Rogers Island to Thompson Island Dam. This reach was discretized using 68 longitudinal and 10 lateral grid cells (QEA, 1999). Average longitudinal grid cell size was 140 m and typical lateral grid cell size was about 20-30 m. Bathymetric data collected in TIP in 1991 were used to specify values of h_o for model input (O'Brien and Gere, 1993). The 1991 bathymetric survey collected depth soundings at about 107,000 points throughout TIP at river flows that ranged from about 48 to 76 m^3/s. The reference water depth (h_o) in each grid cell was calculated by averaging the 1991 sounding data located within that grid cell.

The hydrodynamic model required specification of two types of time-variable boundary conditions: (1) inflows from upstream and tributary sources and (2) stage height at the

dam. Flow rates measured by the U.S. Geological Survey (USGS) at the Fort Edward gauging station were used as input at the upstream boundary of the model. Estimation of tributary discharge to TIP from Snook Kill, Moses Kill and direct runoff was accomplished using a modified drainage area proration method (QEA, 1999). Stage heights measured by Champlain Canal personnel in TIP (T. Rathwell, NYS Thruway Authority, *personal communication* 1996) were used to develop a relationship between flow rate and water surface elevation at the dam. The dam rating curve developed from these data was used to specify the time-variable downstream boundary condition (stage height at Thompson Island Dam) in all simulations.

4. Sediment Transport Model

Generally, relatively simplistic representations of resuspension and deposition processes have been used in past solids transport sub-models associated with contaminant fate models (e.g., O'Connor et al., 1983; Thomann et al., 1993; Velleux and Endicott, 1994). This approach uses non-mechanistic, empirical formulations to simulate resuspension and deposition fluxes at the sediment-water interface, i.e., resuspension and deposition velocities are treated as calibration parameters that can be adjusted temporally and/or spatially. Results from this type of model are typically unsatisfactory and yield predictions that are of questionable value because the sediment dynamics are not accurately and realistically formulated. More sophisticated, mechanistic sediment transport models have been developed and these types of models should be used; contaminant fate models using non-mechanistic solids transport formulations should not be applied in the future.

The sediment transport model used in the present study is a modified version of the SEDZL sediment transport model originally developed by Ziegler and Lick (1986). SEDZL has been used in a number of sediment transport studies, including Fox River in Wisconsin (Gailani et al., 1991), Pawtuxet River in Rhode Island (Ziegler and Nisbet, 1994), Lake Erie (Lick et al., 1994), Saginaw River in Michigan (Cardenas et al., 1995), Buffalo River in New York (Gailani et al., 1996) and Watts Bar Reservoir in Tennessee (Ziegler and Nisbet, 1995).

Suspended sediment particles in a river have a large range of sizes, from less than 1 μm clays to medium sands on the order of 400 μm. Simulation of the entire particle size spectrum is impractical. Therefore, particles were broadly segregated into two groups: silt and clay that may interact and form flocs and sand that is transported as discrete particles. The model uses this approach to approximate the particle size spectrum. "Class 1" particles include all the cohesive particles, i.e., clays and silts, with disaggregated particle diameters of less than 62 μm, while the "class 2" particles include coarser, non-cohesive sediments, primarily fine and medium sand with diameters between 62 and 425 μm. In the past, many contaminant fate models have only used one sediment size class, an approximation that may not produce realistic results. Significant temporal and spatial variations in suspended sediment composition can occur in a river (and do occur in TIP), making it necessary to use at least two sediment size classes.

A two-dimensional, vertically-averaged sediment transport equation for size-class k (k = 1,2) was applied (Ziegler and Nisbet, 1994)

$$\frac{\partial(hC_k)}{\partial t}+\frac{\partial(uhC_k)}{\partial x}+\frac{\partial(vhC_k)}{\partial y}=\frac{\partial}{\partial x}\left(hE_x\frac{\partial C_k}{\partial x}\right)+\frac{\partial}{\partial y}\left(hE_y\frac{\partial C_k}{\partial y}\right)+R_k-D_k \tag{5}$$

where C_k = concentration of suspended sediment of size-class k; E_x, E_y = horizontal eddy diffusivities along the x- and y-axes, respectively; R_k = resuspension (erosion) flux of size-class k; and D_k = deposition flux of size-class k. Results from the hydrodynamic model provide information about the transport field in Equation (5), i.e., u, v and h. Similar to the hydrodynamic equations, Equation (5) has been transformed into an orthogonal, curvilinear coordinate system and solved numerically. The hydrodynamic and sediment transport models used the same numerical grids.

5. Deposition Processes

As mentioned above, cohesive sediments in the water column range from clay particles smaller than 1 μm up to ~62 μm silts. The discrete particles aggregate and form flocs that can vary greatly in size and effective density. Variations in concentration and shear stress affect both floc diameter and settling speed (Burban et al., 1990). Previous modeling studies (Ziegler and Nisbet, 1994, 1995; Gailani et al., 1996) have shown that an effective approximation is to treat suspended cohesive sediments as a single class. This approach assumes that the settling and depositional characteristics of cohesive sediments can be represented by average values of a distribution of properties. Using this approximation, the deposition flux of cohesive (class 1) sediments to the sediment bed is expressed as (Ziegler and Nisbet, 1994)

$$D_1 = P_1 W_{s,1} C_1 \tag{6}$$

where $W_{s,1}$ = cohesive sediment settling speed and P_1 = probability of deposition for cohesive sediments.

Settling speeds of cohesive flocs have been measured over a large range of concentrations and shear stresses in freshwater (Burban et al., 1990). The Burban settling speed data for cohesive flocs in freshwater were analyzed to develop a formulation to approximate the effects of flocculation on settling speed. This analysis indicated that the settling speed is dependent on the product of the concentration (C_1) and the water column shear stress (G) at which the flocs are formed, resulting in the following relationship

$$W_{s,1} = 2.5(C_1 G)^{0.12} \tag{7}$$

where the units of $W_{s,1}$, C_1, and G are m/day, mg/l and Pa, respectively (Figure 2). For a depth-averaged model, as used in this study, the relevant shear stress for use in Equation

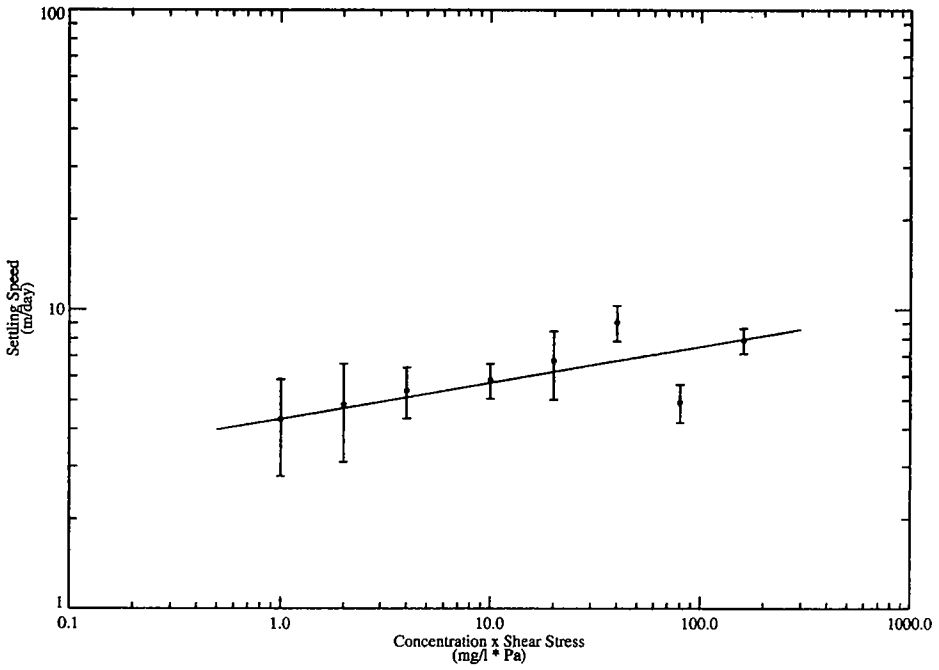

Figure 2. Settling speed function for cohesive (class 1) sediment (solid line) and floc settling speed data (mean ± 95% confidence interval, Burban et al., 1990) used to construct function.

(7) is the bottom shear stress (τ_b), i.e., $G = \tau_b = \rho_w C_f\, q^2$ and ρ_w = water density (assumed to be 1,000 kg/m^3). A previous analysis of the Burban data by Ziegler (Gailani et al., 1991) produced different settling speed formulations than Equation (7). A review of the earlier formulations showed that those equations do not accurately represent the Burban settling speed data. Hence, the present formulation, Equation (7), should be used instead of the equations originally developed by Ziegler (Gailani et al., 1991; Ziegler and Nisbet, 1994, 1995).

Modeling suspended cohesive sediments as a single class, with an effective $W_{s,1}$ given by Equation (7), makes it necessary to use a probability of deposition (P_1) to parameterize the effects of particle/floc size heterogeneity and near-bed turbulence on the deposition rate. The complex interactions occurring in the vicinity of the sediment-water interface cause only a certain fraction of the settling cohesive sediments, represented by P_1, to become incorporated into the bed (Krone, 1962; Partheniades, 1992). An experimentally-based formulation that represents the effects of variable floc size on probability of deposition was developed by Partheniades (1992) (Figure 3)

$$P_1 = 1 - (2\pi)^{-1/2} \int_{-\infty}^{Y} e^{-\frac{w^2}{2}} dw \tag{8}$$

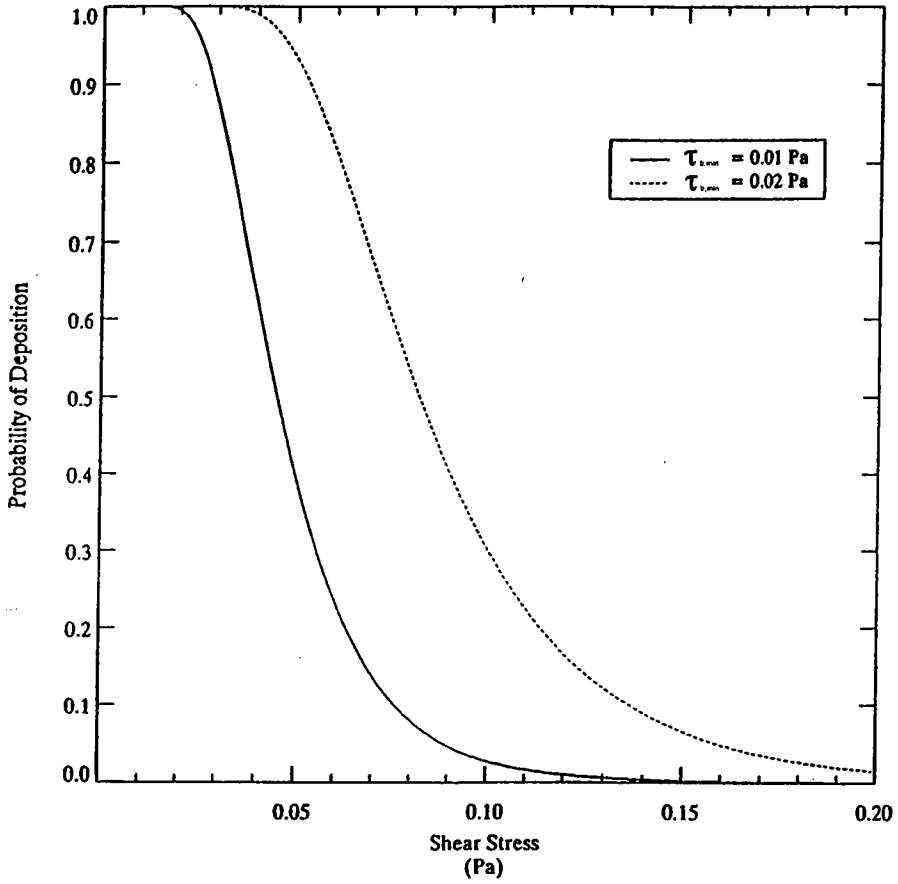

Figure 3. Probability of deposition function for cohesive (class 1) sediment.

where

$$Y = 2.04\ln\left[0.25\left(\frac{\tau_b}{\tau_{b,\min}} - 1\right)e^{1.27\tau_{b,\min}}\right] \tag{9}$$

and $\tau_{b,\min}$ = bottom shear stress below which $P_1 = 1$. A value of 0.01 Pa was used for $\tau_{b,\min}$ and not adjusted during model calibration. This value is consistent with $\tau_{b,\min}$ values reported by Partheniades (1992). Non-mechanistic solids transport sub-models have used a constant effective settling speed (O'Connor et al., 1983; Velleux and Endicott, 1994), an approximation which neglects the important effects of near-bed turbulence on deposition and can produce unrealistic results because significant temporal and spatial variations in τ_b and P_1 occur in any river.

Class 2 particles, i.e., fine and medium sand, suspended in the water column have an effective settling speed ($W_{s,2}$) that depends on the effective particle diameter (d_2). The relationship between $W_{s,2}$ and d_2 was developed by Cheng (1997). The depositional flux for this sediment class is estimated as

$$D_2 = P_2 W_{s,2} \Gamma C_2 \tag{10}$$

where P_2 = probability of deposition for non-cohesive sediments and Γ = class 2 stratification correction factor. Details concerning methods for calculating Γ, $W_{s,2}$ and P_2 are presented in Appendix B. Significant vertical stratification of class 2 sediment can occur in the water column due to the high settling speeds of fine and medium sand. This characteristic means that accurate calculation of class 2 deposition flux requires use of the near-bed concentration ($C_{a,2}$), where $C_{a,2} = \Gamma C_2$ and $\Gamma > 1$. Note that Γ is dependent upon $W_{s,2}$, τ_b, bottom roughness and local depth.

Examination of Equations (6) and (10) shows that the "effective" settling speed of class 1 (P_1 $W_{s,1}$) is typically one to two orders of magnitude lower than that of class 2 ($P_2 W_{s,2}$ Γ). This differential has significant impact on simulation results and underscores the importance of using two sediment size classes as opposed to a single size class as has been typically used in many contaminant fate models.

6. Cohesive Resuspension Processes

Experimental results have shown that a finite amount of material will typically be resuspended from a fine-grained, cohesive sediment bed exposed to a constant bottom shear stress. This phenomenon, referred to as bed armoring, has been observed and quantified in a number of laboratory (Parchure and Mehta, 1985; Tsai and Lick, 1987; Graham et al., 1992) and field studies (Hawley, 1991; Amos et al., 1992). The amount of fine-grained sediment resuspended from a cohesive deposit is (Gailani et al., 1991)

$$\epsilon = \frac{a_o}{T_d^N}\left(\frac{\tau_b - \tau_{cr}}{\tau_{cr}}\right)^n, \tau_b \geq \tau_{cr} \tag{11}$$

where ϵ = net mass of resuspended sediment per unit surface area (resuspension potential); a_o = site-specific constant; T_d = time after deposition in days; N, n = exponents dependent upon the deposition environment; and τ_{cr} = effective critical shear stress. Many contaminant fate models have used a resuspension velocity that is empirically determined during model calibration (O'Connor et al., 1983; Velleux and Endicott, 1994). This procedure can produce highly inaccurate results because: 1) site-specific data are not used to determine erosion parameters (and thus constrain the resuspension process); 2) bed consolidation effects are neglected; and 3) bed armoring effects are not simulated.

Experimental results show that cohesive erosion, for a bed exposed to a constant bottom shear stress, occurs over a time period on the order of one hour, i.e., ϵ mg/cm^2

of sediment are eroded in about one hour (Tsai and Lick, 1987; MacIntyre et al., 1990). Thus, the total resuspension rate ($R_{tot,coh}$) is approximated by

$$R_{tot,coh} = \frac{\epsilon}{3600} \tag{12}$$

where $R_{tot,coh}$ is assumed to be constant until all available sediment is eroded. Once the amount ϵ has been resuspended, $R_{tot,coh}$ is set to zero until additional sediment is deposited and available for resuspension or until the shear stress increases (Gailani et al., 1991). The resuspension rate of class k (R_k) sediment from the cohesive bed is

$$R_k = f_k R_{tot,coh} \tag{13}$$

where f_k = fraction of class k sediment in the surficial layer of the cohesive bed. The present study models two classes of suspendable sediment, with f_1 corresponding to the fraction of cohesive particles (clay and silt) in the bed and f_2 representing the fraction of suspendable non-cohesive particles (fine and medium sand with particle diameters between 62 and 425 μm). The total fraction of suspendable sediment in the bed ($f_{sus} = f_1 + f_2$) is equal to one in the cohesive bed. In non-cohesive bed areas, f_{sus} can be less than or equal to one, depending on local conditions.

The effects of bed consolidation with depth and horizontal variations in bed composition are simulated using a three-dimensional model of the cohesive sediment bed. The layered bed model conserves mass, with mass flux occurring only at the sediment-water interface due to deposition and resuspension. Vertical variations of sediment bed consolidation, or equivalently porosity, are accounted for by discretizing the bed into seven layers. The time after deposition of the layers increases linearly from one day at the surface, which is composed of freshly deposited sediment, to seven days in the bottom layer. Previous laboratory studies (Tsai and Lick, 1987; MacIntyre et al., 1990) indicate that consolidation effects on resuspension are minimal after about seven days of consolidation. Therefore, the maximum age of deposited sediments was set at seven days. Consolidation effects on resuspension are accounted for in Equation (11) by the $(T_d)^{-N}$ term, which causes the resuspension potential (ϵ) to decrease as the bed consolidates with time. The critical shear stress, τ_{cr}, was assumed to be constant in all layers of the bed. The model accounts for changes in bed composition, i.e., f_1 and f_2, due to resuspension and deposition during the course of a simulation.

7. Non-Cohesive Resuspension Processes

Simulation of non-cohesive resuspension in TIP is necessary because: 1) non-cohesive bed areas, composed primarily of sand and gravel, represent over 75% of the TIP sediment bed and 2) cohesive and non-cohesive resuspension processes are very different. Typically, non-mechanistic solids transport sub-models have not accounted

for spatial variations in resuspension properties and have used a spatially constant resuspension velocity. This approach would not be adequate for TIP (nor the rest of the UHR) and, generally, it should not be applied to other rivers.

The non-cohesive suspended load transport model developed by Ziegler and Nisbet (1994), and applied to the Pawtuxet River (Rhode Island), was modified and enhanced for application to TIP. The resuspension of sediment from the non-cohesive portion of the sediment bed in TIP was calculated using a procedure developed by van Rijn (1984), see QEA (1999) for details. The van Rijn method has been shown to yield good results for predicting suspended load transport of sands (van Rijn, 1984; Garcia and Parker, 1991; van Rijn et al., 1993). Resuspension of class 1 sediment from the non-cohesive bed was calculated using an effective diameter of 50 μm (silt) in the van Rijn equations. For class 2 sediment, the effective diameter used in the van Rijn formulations was d_2, the value of which was determined through model calibration.

Non-cohesive areas of the sediment bed in TIP typically contain a significant fraction of non-suspendable coarse sand and gravel. When erosion occurs in these areas, the suspendable sediment in the near-surface layer, referred to as the active layer, is depleted. Continuous depletion of suspendable sediment in the active layer will eventually reduce the erosion rate to zero. At this point, the active layer is composed entirely of non-suspendable sediment, and the sediment bed has become armored (Karim and Holly, 1986; Jain and Park, 1989; van Niekerk et al., 1992).

The bed armoring process has been modeled by assuming that the sediment bed is composed of an active layer, which interacts with the water column, and a parent bed, which is below the active layer (Karim and Holly, 1986; van Niekerk et al., 1992). Interactions between the parent bed, active layer and water column cause the grain size distributions in the active layer and parent bed to change with time. Tracking temporal and spatial changes of class 1 and 2 volumes in the active and parent bed layers is accomplished using the bed model proposed by Karim and Holly (1986). The two-layer bed model conserves mass, with deposition and resuspension fluxes at the sediment-water interface being the only gain or loss mechanism for the non-cohesive bed.

The thickness of the active layer is of critical importance in applying this model. Various formulations have been proposed for the active layer thickness, e.g., Borah et al. (1982), Karim and Holly (1986) and Jain and Park (1989). An expression for the active layer thickness, which is a linear function of the local bottom shear stress, was developed by van Niekerk et al. (1992). A modified form of their formulation was used in this study

$$T_a = \begin{cases} 2d_{50} & , \quad \tau_b < \tau_{c50} \\ 2d_{50}\left[B\left(\frac{\tau_b}{\tau_{c50}}\right) + (1 - B)\right] & , \quad \tau_b \geq \tau_{c50} \end{cases} \tag{14}$$

where T_a = active layer thickness; d_{50} = median particle size of bed sediment; τ_{c50} = critical shear stress for initiation of bed load based upon the parent bed d_{50}; and B = adjustable constant. Note that Equation (14) reduces to the original van Niekerk et al. (1992) equation

when B is equal to 1. Varying hydrodynamic conditions affect the active layer thickness, with T_a increasing as the current velocity (and τ_b) increases, which causes the amount of sediment that is available for resuspension to increase. The dependence of T_a on τ_b is not well known and the constant (B) in Equation (14) was adjusted during model calibration to account for local conditions in TIP.

8. Specification of Bed Properties

Accurate determination of bed property parameters is of critical importance, particularly because of the heterogeneous structure of the TIP sediment bed. A large quantity of bed property data is available for TIP. Sediment bed maps, developed using data from a side-scan sonar survey conducted by USEPA in TIP (Flood, 1993), were used to characterize the sediment of each model grid cell as cohesive, non-cohesive or hard bottom. Cohesive sediment bed areas in TIP correspond to 22% of the total area of this reach. Bulk bed property data for TIP cohesive sediments exhibit no definite spatial trends. Therefore, average values, determined from surficial core data collected in TIP, were used to specify the dry density (0.87 g/cm^3) and initial composition (f_1 = 0.32) in the cohesive bed areas. An average dry density of 1.38 g/cm^3 was applied to non-cohesive sediments. Analysis of TIP *in situ* resuspension potential data indicated that an appropriate value for the exponent n in Equation (11) is 2.94. TIP data also exhibited a spatial variation in the site-specific constant, a_o, with values ranging from 0.035 to 0.239 mg-day$^{1/2}$/cm^2. Laboratory experiments on the resuspension characteristics of TIP cohesive sediments indicated that appropriate values for τ_{cr}, N and $T_{d,\max}$ were 0.1 Pa, 0.5 and 7 days (QEA, 1999).

The non-cohesive suspended load transport model required specification of median particle diameter (d_{50}) and suspendable sediment fractions (i.e., f_1 and f_2) in the non-cohesive bed. Determination of spatial and temporal changes in d_{50} was needed for calculation of T_a using Equation (14). Because the model is sensitive to local values of d_{50}, f_1 and f_2 and data for these quantities are highly variable, it was necessary to develop a procedure for estimating local values from the available data. This methodology can be used for specifying spatial distributions of non-cohesive bed properties in other rivers.

The spatial distribution of d_{50} was estimated on the basis of a relationship between local bottom shear stress and d_{50}, i.e., $d_{50} = f(\tau_b)$. The hydrodynamic model was used to predict the bottom shear stress distribution for the non-cohesive bed at a given flow rate (849 m^3/s). The functional relationship between d_{50} and τ_b was determined by iterative adjustment until the predicted and measured distributions of d_{50} were in general agreement (QEA 1999). The resulting function is (for d_{50} in μm)

$$\begin{aligned} d_{50} &= 140e^{16.6\tau_n^2} \quad , \quad \tau_n < 0.45 \\ &= 9000\tau_n^{1.02} \quad , \quad \tau_n \geq 0.45 \end{aligned} \tag{15}$$

where τ_n = normalized bottom shear stress (τ_b/τ_{max}) and τ_{max} = maximum bottom shear stress in non-cohesive bed area at given flow rate (4.7 Pa at 849 m^3/s). A log-linear correlation between f_2 and d_{50} was observed in TIP bed data

$$f_2 = 22\ d_{50}^{-0.66} \tag{16}$$

Predicted d_{50} values, from Equation (15), were used in Equation (16) to generate the initial spatial distribution of f_2 in TIP. The average predicted and measured f_2 values in TIP non-cohesive bed area were 0.29 and 0.34, respectively. Non-cohesive bed data did not indicate a strong relationship between d_{50} and f_1. Thus, an average initial f_1 value of 0.065 was used throughout TIP non-cohesive bed. The spatial distributions of d_{50}, f_1 and f_2 that were estimated using the above procedure are initial conditions for the model. The non-cohesive sediment bed model tracks temporal changes in f_1 and f_2 in each grid cell due to resuspension and deposition.

A relationship between median particle diameter (d_{50}) and fraction of suspendable sediment ($f_{sus} = f_1 + f_2$) in the non-cohesive bed was determined from grain size distribution data collected from TIP

$$d_{50} = 135 f_{sus}^{-1.67} \tag{17}$$

where d_{50} has units of μm. This data-based relationship between d_{50} and f_{sus} was used to dynamically adjust d_{50} during a simulation, i.e., as f_1 and f_2 vary temporally at a particular location due to resuspension and deposition, d_{50} is adjusted.

9. Specification of Sediment Loading

Sediment loading is of primary importance for any contaminant fate study in a riverine system. The reason for this emphasis is that net sedimentation (burial) rates are significantly affected by solids loads entering a river. Burial rates are a controlling factor in determining the rate of change of contaminant concentration in the bioavailable layer of the sediment bed, which is usually a focus of remedial alternative investigations. Therefore, significant data collection and analysis efforts should be directed at accurate determination of sediment loads to the river. Sufficient data were available to accurately estimate TIP sediment loads from upstream and tributary sources for short-term and long-term simulations.

Sediment loading at the upstream boundary of the model (Fort Edward) and from TIP tributaries were estimated using total suspended sediment (TSS) concentration data collected at those locations. Sediment rating curves, which relate TSS concentration to flow rate, were developed for the Hudson River at Fort Edward, Snook Kill and Moses Kill (QEA, 1999). Fort Edward sediment loads were specified using TSS concentration data when data were available; the rating curve was used to estimate TSS concentration at that location when data were not available. Sediment loading from TIP direct drainage was

estimated using a rating curve that was the average of the rating curves for Snook and Moses Kills. The tributary rating curves produced a sediment yield of 20 tons/yr-km^2 for the TIP drainage basin.

The USGS collected particle size distribution data for suspended sediments at three UHR locations downstream of TIP. Analysis of the data showed no correlation existed between sand content and flow (or TSS concentration) at the three UHR locations. The sand content data at the three sampling locations had mean values that ranged from 16 to 26%. Based on these data, the assumption was made that the sand content of sediment loads at Fort Edward and Snook Kill was 25% for all flows rates. The sand content of sediment loads from Moses Kill and direct drainage runoff was assumed to be zero. The hydraulic characteristics of these two sediment sources prevent the transport of significant quantities of sand into TIP.

10. Hydrodynamic Model Calibration and Validation

The hydrodynamic model contains two parameters that can be adjusted during the model calibration process: horizontal eddy viscosity (B_H) and effective bottom roughness (z_o). The hydrodynamic model was run with the minimum value of B_H needed to ensure numerical stability, which was 0.5 m^2/s for TIP. No further adjustment of B_H was made during model calibration or validation. Values of z_o and $C_{f,\min}$ depend on local bed type, i.e., cohesive, non-cohesive or hard bottom (rocky). For all cohesive areas in TIP, z_o and $C_{f,\min}$ were set at 75 μm and 0.0020, respectively, and were not adjusted during calibration. Optimum values for the bottom friction coefficients in non-cohesive/hard bottom areas were determined by model calibration.

Champlain Canal stage height data collected at Gauge 119, located near the lock entrance at Fort Edward, were used to develop a rating curve at this location, similar to the stage height rating curve generated at Thompson Island Dam. Calibration of the hydrodynamic model in TIP was accomplished by comparing predicted water surface elevations near Fort Edward to stage heights estimated from the Gauge 119 rating curve. A range of flows, from 71 to 991 m^3/s (2,500 to 35,000 cfs) was used to predict water surface elevations at the Gauge 119 location. The bottom friction coefficients were adjusted until the average error over the flow range was minimized. The best calibration results were achieved with z_o = 1,500 μm and $C_{f,\min}$ = 0.0035 in the non-cohesive/hard bottom areas. An average error of 4% resulted for these parameter values over the flow range of 71 to 991 m^3/s.

The hydrodynamic model was validated using water surface elevation data obtained at Gauge 119 during the 1983 spring flood in TIP. This flood had a maximum flow rate at Fort Edward of 965 m^3/s (34,100 cfs), which represents a return period of approximately 10 years. Effective bottom roughness (z_o) was not adjusted during model validation, only model boundary conditions were changed. The model validation results are shown in Figure 4. Agreement between predicted and measured stage heights during this flood was excellent. In addition, the hydrodynamic model was validated using velocity data collected along five TIP transects during low-flow conditions in August 1997. Model-data

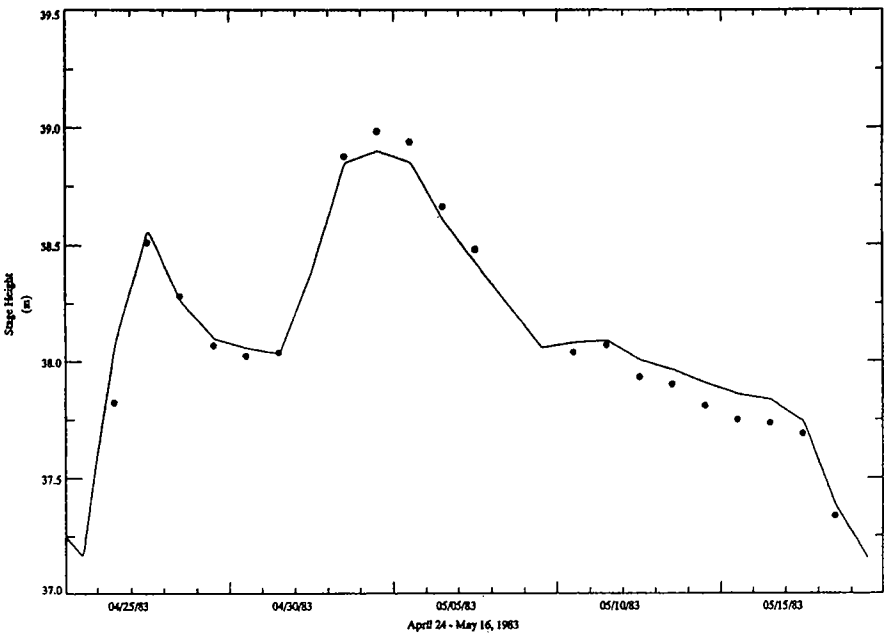

Figure 4. Comparison of predicted (solid line) and observed TIP stage heights at Gauge 119 during 1983 spring flood.

comparisons were fair (QEA, 1999), with discrepancies probably due to poor grid resolution in the sampling area (which was near a group of islands near Snook Kill). Successful calibration and validation of the model demonstrates that: (1) model geometry and bathymetry are adequately represented and (2) bottom friction factors used in the model are realistic. However, some uncertainty exists in the capability of the model to accurately represent lateral variations in current velocity.

11. Sediment Transport Model Calibration

The longitudinal eddy diffusivity (E_x) was set equal to the eddy viscosity (B_H) used in the hydrodynamic model (0.5 m^2/s). Initial model testing, using data and observations from the 1997 spring flood, indicated that the model produced more realistic results in TIP when an anisotropic eddy diffusivity was used. The lateral eddy diffusivity (E_y) was reduced to 0.05 m^2/s to improve qualitative agreement between predicted and observed patterns of suspended sediment plumes from Snook and Moses Kills during the 1997 spring flood. Adjustment of E_y was done prior to model calibration; no adjustment of this parameter was made during the calibration process.

The sediment transport model was calibrated using TSS concentration data collected during the 1994 spring flood. A mass balance assessment and TSS concentration comparisons were used to calibrate the model and to evaluate the resuspension and deposition formulas. The 30-day calibration period extended from March 31 through April 29, 1994. The maximum daily average flow rate at Fort Edward during this period was 784 m^3/s (27,700 cfs). This period was unique because TSS concentration data were collected at Fort Edward, Snook Kill, Moses Kill and three locations in TIP (USEPA, 1995).

Model calibration involved determining a consistent set of values for the following four parameters: (1) d_2, the effective diameter of suspended class 2 particles; (2) B, the constant in the non-cohesive bed active layer thickness equation; (3) d_{50}(x,y), the spatially variable median diameter of sediment in the non-cohesive bed; and (4) f_2(x,y), the spatially variable fraction of class 2 sediment in the non-cohesive bed. Only d_2 and B were adjusted during model calibration. The model calculated spatial and temporal changes in d_{50}, f_1 and f_2. However, changes in d_2 and B values can affect the predicted distributions of d_{50}, f_1 and f_2.

Initial values for d_{50}(x,y) and f_2(x,y) were generated using Equations (15) and (16). Determination of consistent parameter values involved finding values of d_2 and B that produced accurate erosion and deposition fluxes for bed characteristics (d_{50} and f_2) expected to exist at the time of the calibration flood. An iterative procedure was used to calibrate the model whereby long-term simulations, from 1977 to 1994, were used to determine non-cohesive bed properties (d_{50}, f_1 and f_2) at the beginning of the calibration period, during which d_2 and B were adjusted to minimize model error (QEA, 1999). Best model-data agreement was found using d_2 and B values of 90 μm and 0.016, respectively. A value of 90 μm for d_2 corresponds to very fine sand and is a realistic value of the effective diameter of suspended class 2 particles. Very fine sand with a particle diameter of 90 μm has a settling speed of about 400 m/day (approximately two orders of magnitude greater than $W_{s,1}$). The non-cohesive bed armoring constant (B = 0.016) has no physical basis but the low B value indicates that the active layer thickness (T_a) was weakly dependent on bottom shear stress in TIP.

The calibration process involved comparing predicted and observed TSS concentrations at three locations in TIP: (1) upstream of Snook Kill; (2) McDonald's dock; and (3) Thompson Island Dam (see Figure 1 for locations). Results of the final calibration are presented in Figure 5. Generally, the model agreed very well with observed TSS concentration at all three locations in TIP.

Comparisons between predicted and observed TSS are a typical method of calibrating and validating a sediment transport model (e.g., Gailani et al., 1991; Ziegler and Nisbet, 1994). However, this method does not necessarily ensure that the model realistically and accurately simulates resuspension and deposition fluxes in TIP. The reason for this uncertainty is that external sediment loadings, from upstream and tributary sources, may dominate predicted and observed TSS concentrations in TIP, with deposition and resuspension causing relatively small changes in water column sediment concentrations. Large changes in model parameters, creating large changes in deposition and resuspension, may cause relatively small changes in predicted TSS concentrations.

To reduce the uncertainty in model parameterization of deposition and resuspension processes, and thus to improve the predictive capabilities of the sediment transport model,

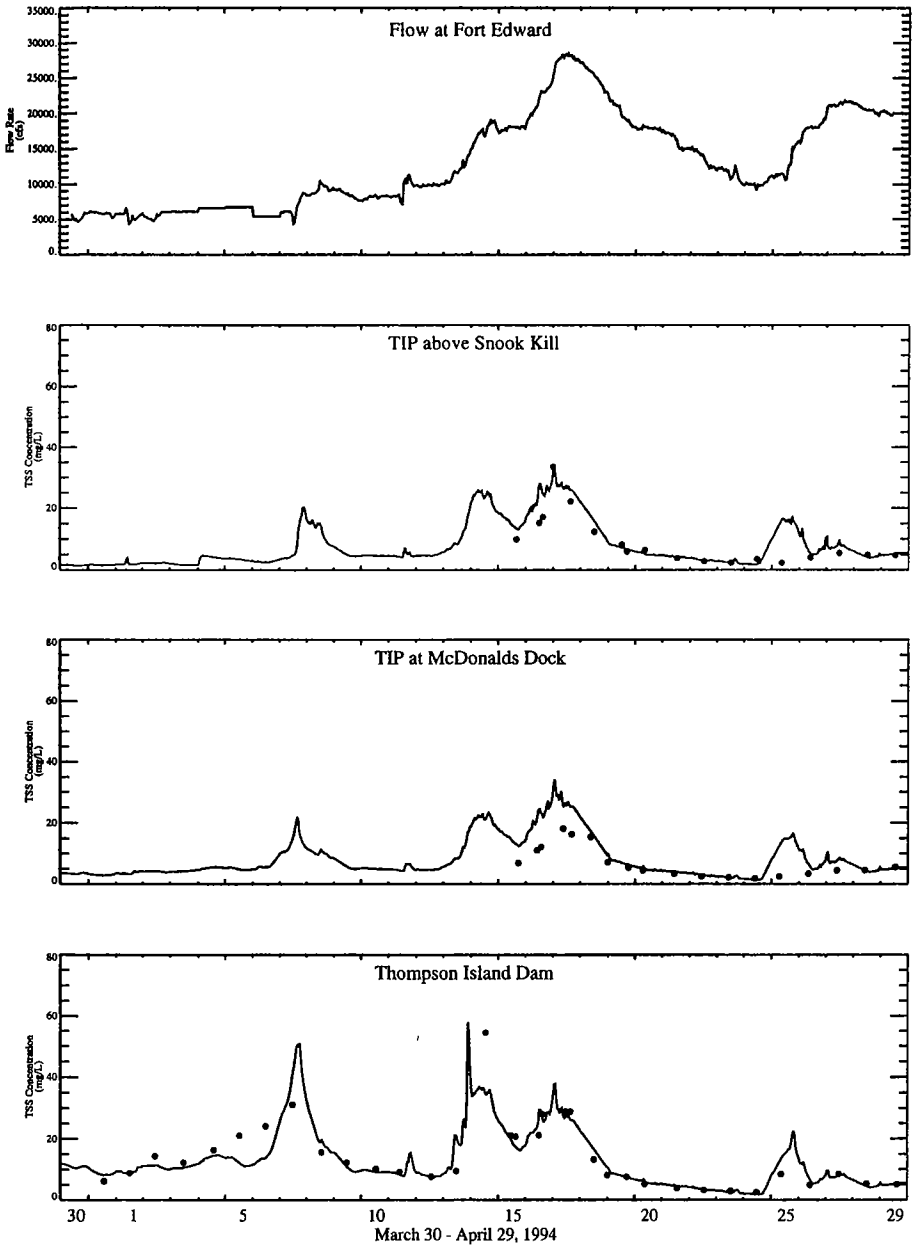

Figure 5. Comparison of predicted (solid line) and observed TSS concentrations at three locations in the TIP during the 1994 spring flood.

an additional calibration procedure was developed. This procedure involved constructing a sediment mass balance for TIP, using the total sediment load input from upstream and tributary sources (L_{in}) and the output sediment load at Thompson Island Dam (L_{out}), to calculate the net resuspension/deposition in TIP. A sediment mass balance for TIP during a particular period is expressed as: $L_{in} - L_{out} = \Delta M_{wc} + M_{dep} - M_{res}$, where ΔM_{wc} = change in total suspended sediment mass, M_{dep} = deposition mass and M_{res} = resuspension mass. Net flux to the sediment bed (M_{bed}) was calculated using: $M_{bed} = L_{in} - L_{out} - \Delta M_{wc} = M_{dep} - M_{res}$. Thus, for a given time period, net deposition occurs if $M_{bed} > 0$ and net resuspension occurs if $M_{bed} < 0$. Note that this type of data analysis can only estimate global losses or gains due to net erosion or deposition from TIP sediment bed. This analysis cannot be used to infer net erosion or deposition in specific bed types, e.g., cohesive or non-cohesive, or areas of TIP.

Sufficient data were collected during the 30-day period from March 31 through April 29, 1994 to develop estimates of M_{bed} on an hourly basis. Note that it was assumed for all mass balances, during calibration and validation simulation periods, that the model was the best estimator of the change in sediment mass suspended in the water column of TIP (ΔM_{wc}). So, predicted ΔM_{wc} values were used to complete all mass balances for a particular period. Generally, ΔM_{wc} was small compared to the quantity ($L_{in} - L_{out}$), i.e., less than 5%, so using predicted ΔM_{wc} in the data-based mass balance did not introduce significant error.

The results of this data analysis showed that net erosion occurred during the 30-day period and that 450 tons of sediment were transported out of TIP. The model predicted that a total of 370 tons of sediment were exported from TIP during this period, which is 18% lower than the data-based estimate. Further examination of data indicated that the period could be separated into two distinct sub-periods: (1) tributary deposition and (2) main stem flood. From March 31 to April 10, flow rates in the Hudson River were non-flooding (< 283 m^3/s) but high flow events occurred in the tributaries. Snook and Moses Kills transported large quantities of sediment into TIP during this sub-period and, because flow rates in the UHR were relatively low, significant deposition occurred. The data-based mass balance indicated that 390 tons of sediment were deposited during the tributary deposition sub-period. The model predicted 530 tons of deposited sediment, corresponding to a 36% over-prediction when compared to the observed value. Net erosion occurred during the main stem flood sub-period (April 11 to 29) with 840 tons of sediment lost from TIP. The model was within 7% (900 tons) of the data-based estimate of net erosion during the main stem flood sub-period.

12. Sediment Transport Model Validation

Model performance was validated using two simulation periods: (1) 1997 spring flood and (2) long-term, 1977 to 1998. No adjustment of model parameters was made during these validation simulations, only boundary conditions, e.g., inflows and sediment loads, were changed. The 1997 spring flood results provide additional confidence in the capability of the model to simulate short-term, high flow events. The long-term simulation demon-

strated that the model accurately predicted TSS concentrations at Thompson Island Dam and sedimentation rates in cohesive bed areas.

The spring flood that occurred in early May 1997 had a relatively low peak flow, with a maximum flow rate at Fort Edward of approximately 510 m^3/s (18,000 cfs). TSS concentration data were collected at Fort Edward, Snook Kill, Moses Kill and Thompson Island Dam between April 25 and May 7, which was the period when a high flow event occurred on Snook and Moses Kills. Comparisons of predicted and observed TSS concentrations at Thompson Island Dam during this eleven-day period are shown in Figure 6. Model results were in good agreement with measured TSS concentrations on both the western and eastern shores of the dam. Similar to the 1994 spring flood, a mass balance approach was used to evaluate model performance for the 1997 spring flood. A seven-day period, from April 28 to May 4, was used for the mass balance because high frequency data were available during this period. The data-based mass balance indicated that net erosion occurred in TIP, with 450 tons of sediment transported out of this reach. The model is in excellent agreement, with 470 tons of net erosion being predicted during the mass balance period, corresponding to a 4% error.

As discussed previously, long-term calculations were performed iteratively as part of the model calibration process. A final long-term simulation was conducted to further validate the sediment transport model. This calculation was almost 22 years long, starting on January 1, 1977 and ending on December 9, 1998. Comparisons of observed and predicted sedimentation rates in TIP were made as an evaluation of long-term performance. Three high-resolution sediment cores were collected in 1992 by USEPA in TIP. Geochronologic dating, using ^{137}Cs concentration data, of those cores indicated average sedimentation rates that ranged between 0.9 and 1.2 cm/yr. Model-to-data comparisons at these locations were 0.5 to 0.9, 1.1 to 1.2 and 1.7 to 0.9 cm/yr. The last comparison was between the sampled location and the model grid cell just upstream of that location. The grid cell at the matching location exhibited net erosion. The model-data comparison at the first location improves to 0.95 to 0.9 cm/yr if the grid cell just upstream of the core location is used. These differences can be attributed to uncertainty in bed mapping and grid resolution. These results demonstrate that the model is not biased high or low and that the model predicts deposition rates within a factor of two of measured values, providing added confidence that the sediment transport model can simulate long-term TIP deposition rates.

Further validation of the sediment transport model is provided by results from the PCB fate and transport model (Connolly et al., 2000). Long-term changes in surficial PCB bed concentrations are primarily determined by burial rates, which are controlled by sediment transport processes. The PCB fate model was able to predict long-term (1977 to 1998) declines in surficial bed concentrations with high accuracy in cohesive and non-cohesive bed areas of TIP. Furthermore, within a specific bed type, i.e., cohesive or non-cohesive, significant spatial variability in natural attenuation rates was indicated by the data and the model was able to reproduce this spatial variability (Connolly et al., 2000). These results strongly support the scientific credibility of the sediment transport model (as well as the PCB fate model) and demonstrate its usefulness.

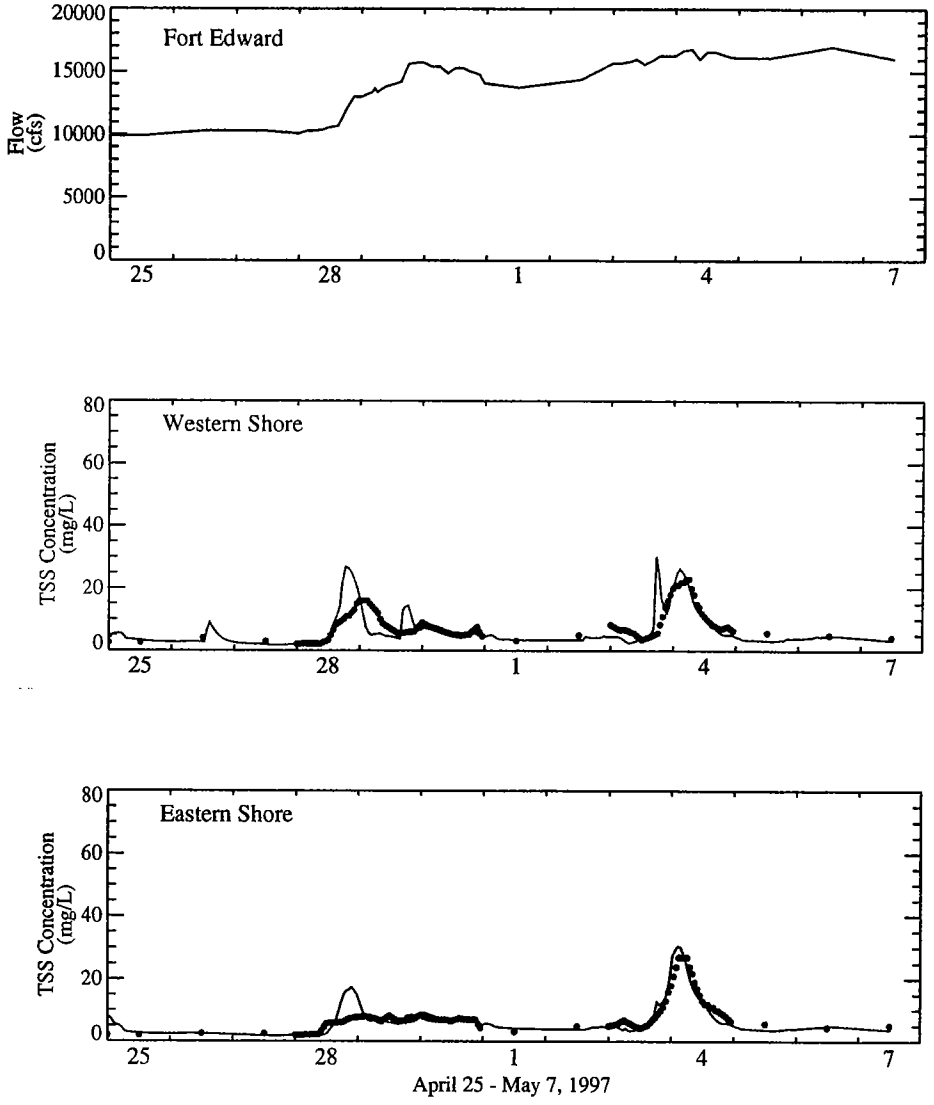

Figure 6. Comparison of predicted (solid line) and measured TSS concentrations at Thompson Island Dam during the 1997 spring flood.

13. TIP Sediment Transport Processes

Successful calibration and validation of the hydrodynamic and sediment transport models indicates that the models can be used as a diagnostic tool to better understand sediment

transport processes in TIP. Increased knowledge of sediment transport dynamics in this reach is important when studying PCB fate and evaluating potential remedial alternatives.

Mass balance analyses, based on model predictions, for TIP during the 1994 (784 m^3/s peak flow) and 1997 (~510 m^3/s peak flow) spring floods indicate that net deposition occurred in the cohesive bed areas, even though net erosion occurred within the entire TIP. These results are consistent with the concept of episodic deposition, where significant deposition occurs during floods and relatively minor deposition occurs during non-flooding periods, e.g., 90% of the annual deposition may happen during 10% of the year (Ager, 1981). Net deposition in TIP cohesive bed area during these floods is consistent with observed depositional patterns in fine-grained areas of the Upper Mississippi River during major flooding in 1993 (Barber and Writer, 1998).

Performing a sediment mass balance on TIP showed that the model predicted 69,600 tons of sediment were deposited during the period from May 1, 1977 through December 9, 1998, which corresponds to a long-term trapping efficiency of 9% for TIP. Most of the deposition occurred in the cohesive bed areas of the pool, with 87% (nearly 60,200 tons) being deposited in those areas. This amount of deposition translates to an average sedimentation rate of 0.81 cm/yr for the cohesive bed in TIP. Even though net deposition occurred in only 36% of the non-cohesive bed area, average net deposition, at the relatively low rate of 0.027 cm/yr, was predicted over this area.

The modeling results discussed above show that net sedimentation, at varying rates, is occurring over most of TIP cohesive sediment bed. This result has important implications for the fate of PCBs in this reach of the UHR because it implies that burial is a major loss mechanism for PCBs in the bioavailable zone of the sediment bed. The consequences of this finding, and its impact on PCB fate and the efficacy of various remedial options, is discussed in further detail in QEA (1999) and Connolly et al. (2000).

Another conclusion based on modeling results is that non-cohesive bed areas are important contributors to sediment transport within TIP. Clay, silt and fine sand (fine-grained sediments) are deposited in the non-cohesive bed during low to moderate flows. These fine-grained sediments may be resuspended during high flow events and transported downstream. Additionally, a portion of the fine sand resuspended from the non-cohesive bed during high flow events is re-deposited in downstream cohesive bed areas, which are generally located in relatively low-energy depositional environments. Thus, the non-cohesive bed effectively serves as a temporary storage reservoir for coarser suspended sediment; fine sand accumulates during low to moderate flows and is released back to the water column during high flow events, contributing to deposition in downstream cohesive bed areas. Cohesive sediment particles (clay and silt) deposited in non-cohesive bed areas erode and are transported downstream during floods. However, in contrast to fine sand re-deposition, significantly less re-deposition of the eroded cohesive particles occurs because of the depositional characteristics of this sediment type. A large fraction of the cohesive sediment particles within the surficial layer of the non-cohesive bed is resuspended during high flow events. Therefore, non-cohesive bed areas serve as a temporary storage area for cohesive sediment particles between floods. Thus, long-term accumulation of PCBs associated with cohesive sediment particles does not generally occur in the non-cohesive bed of TIP.